The proteomic landscape of resting and activated CD4+ T cells reveal insights into cell differentiation and function

Yashwanth Subbannayya[1], Markus Haug[1], Sneha M. Pinto[1], Varshasnata Mohanty[2], Hany Zakaria Meås[1], Trude Helen Flo[1], T.S. Keshava Prasad[2] and Richard K. Kandasamy[1,*]

[1]Centre of Molecular Inflammation Research (CEMIR), and Department of Clinical and Molecular Medicine (IKOM), Norwegian University of Science and Technology, N-7491 Trondheim, Norway
[2]Center for Systems Biology and Molecular Medicine, Yenepoya (Deemed to be University), Mangalore, India

*Correspondence to:

Professor Richard Kumaran Kandasamy
Norwegian University of Science and Technology (NTNU)
Centre of Molecular Inflammation Research (CEMIR)
PO Box 8905 MTFS
Trondheim 7491
Norway
E-mail: richard.k.kandasamy@ntnu.no (Kandasamy R K)
Tel.: +47-7282-4511

Abstract

CD4+ T cells (T helper cells) are cytokine-producing adaptive immune cells that activate or regulate the responses of various immune cells. The activation and functional status of CD4+ T cells is important for adequate responses to pathogen infections but has also been associated with auto-immune disorders and survival in several cancers. In the current study, we carried out a label-free high-resolution FTMS-based proteomic profiling of resting and T cell receptor-activated (72h) primary human CD4+ T cells from peripheral blood of healthy donors as well as SUP-T1 cells. We identified 5,237 proteins, of which significant alterations in the levels of 1,119 proteins were observed between resting and activated CD4+ T cells. We confirmed several known T-cell activation-related processes such as IL-2 response, metabolic and signaling changes, cell cycle induction, differentiation into effector cells among others. Several stimulatory/inhibitory immune checkpoint markers were altered considerably between resting and activated CD4+ T cells. Network analysis identified several known regulatory hubs of CD4+ T cell activation, including IFNG, IRF1, FOXP3, AURKA, and novel hubs such as RIOK2. Comparison of primary CD4+ T cell proteomic profiles with human lymphoblastic cell lines revealed a substantial overlap, while comparison with mouse CD+ T cell data suggested interspecies proteomic differences.

Keywords: adaptive immunity, T-lymphocytes, CD4+ T helper cells, mass spectrometry, proteomics, label-free quantitation, systems biology

Introduction

CD4+ T cells, also known as CD4+ T helper cells, are a subtype of T-lymphocytes that perform important immunoregulatory roles in adaptive immunity, including activation of B cells, cytotoxic T-cells, and nonimmune cells [1]. Bone marrow-derived hematopoietic progenitors committed of the T-cell lineage, unlike other cells of the hematopoietic cell lineage, enter circulation and migrate to the thymus and undergo maturation and selection processes to produce a pool of mature resting CD4+ and CD8+ T cell lineages [2]. During maturation, each T cell re-arranges a unique T cell receptor (TCR) that recognizes specific antigenic peptides in complex with major histocompatibility complex (MHC) molecules on antigen-presenting cells (APCs). Mature naïve T cells exit the thymus and patrol the blood and lymph system where they screen MHC molecules on APCs and are activated if their TCRs detect their cognate antigen on MHC molecules [3]. In addition, subsequent signals, including costimulatory receptor signaling (e.g. CD28) and environmental impacts such as cytokines, are essential for T cell activation [4]. The interactions between APCs and T cells are mediated by regulatory molecules known as immune checkpoints [5]. After activation, CD4+ T cells undergo clonal expansion and differentiation into CD4+ effector T cells. During this phase, cytokine signals from the environment impact the transcriptional programs in the activated CD4+ T cells and guide differentiation towards CD4+ T cell lineages which produce specific sets of effector cytokines. In 1986, Mosmann and colleagues identified two distinct types of CD4+ T helper cells: Type1 T helper cells (Th1) that produced IL-2, IL-3, IFNγ, and GM-CSF, and Type2 T helper cells (Th2) that produced IL-3, BSF1 (IL-4), a mast cell growth factor (IL-10) and a T cell growth factor [6]. However, over the years, multiple/a variety of subsets or lineages of CD4+ T helper cells have been identified depending upon their signature cytokine secretion, which includes -Th1, Th2, Th17, Th9, Th22, regulatory T cells (Tregs), and follicular helper T cells (TFH) [7, 8]. Distinct transcriptional profiles and master transcriptional regulators have been identified for the different subsets/regulating lineage differentiation [9, 10]. It is now understood that not all activated CD4+ T helper cells terminally differentiate, but that a substantial portion remains plastic and may be capable of acquiring other properties and functions as part of secondary immune responses [7].

CD4+ T cells play critical roles in the pathogenesis of several diseases, including infectious, auto-immune, inflammatory diseases, and malignancies. CD4+ T cells have a crucial role in the development of HIV infection, where virus entry into cells requires CD4 receptor involvement [11, 12]. Progressive depletion of CD4+ T cell populations is one of the hallmarks of acquired immunodeficiency syndrome (AIDS) pathogenesis [13] resulting in increased susceptibility to opportunistic infections and virus-associated malignancies [14]. Interestingly, an increase in various CD4+ T cell subsets serves as a hallmark of inflammatory diseases such as multiple sclerosis, arthritis, allergies, and chronic airway inflammation in asthma [15], and infiltration and accumulation of CD4+ T cells in the peripheral joints is an important feature of rheumatoid arthritis [16]. Additionally, CD4+ T cells play an important role in mediating crosstalk between immune cells and adipose tissues with an increase in adipose tissues known to be associated with obesity and obesity-associated diseases, including type 2 diabetes, insulin resistance, atherosclerosis, and stroke [17]. Increasing evidence now suggests a vital role of CD4+T cells in tumor protection [18], driving several anti-tumor mechanisms [19-22]. Furthermore, CD4+ T cells have been shown to mediate direct cytotoxicity against tumor cells through increased production of interferon gamma (IFNγ) and tumor necrosis factor (TNFα in both preclinical models [23-25] and patient-derived CD4+ T cells [26]. CD4+ T cells can also induce humoral responses against tumor antigens primarily through increased expression of CD40 ligand that promotes

differentiation and maturation of B-cells into affinity-matured, class-switched plasma cells [27, 28].

T cell activation is accompanied with changes in transcriptional and proteomic machinery, including massive shifts in metabolism and biosynthesis which drives increase in size, rapid proliferation and differentiation of T cells [29]. To date, there have been several OMICs-based studies, specifically proteomics approaches to characterize changes in protein expression upon T cell activation [30-35]. Despite CD4+ T cells studied extensively, several aspects pertaining to T cell biology, such as comprehensive knowledge of the proteomic repertoire, signaling mechanisms, patterns of heterogeneity in the population, interspecies differences, and fundamental differences between primary cells and cell line models, are not well characterized. The aim of this study was to add knowledge to the proteomic differences between resting and *in vitro* activated primary human CD4+ T cells as well as common laboratory-used model T cell lines. We carried out label-free comparative proteomic analysis of resting (unactivated) and TCR-activated (72 hours) primary human CD4+ T cells purified from two healthy donors. Furthermore, we also profiled the proteome expression repertoire of the human T cell lymphoblastic cell line SUP-T1 and accessed a previously published proteome profile of Jurkat T lymphoblast cells [36]. Using an integrative bioinformatics approach, we compared the proteomic profiles of resting and activated primary CD4+ T cells with those of human SUP-T1 and Jurkat T lymphoblast cell lines. We also provide a comprehensive overview of signaling pathways and networks affected by the activation of CD4+ T cells. The data generated from the current study will enable us to gain a better understanding of the molecular machinery operating within primary CD4+ T cells during T cell activation, the proteomic differences between primary CD4+ T cells and model T cell lines as well as interspecies differences between human and mice.

Results

Comparative proteomic analysis of resting and activated primary CD4+ T cells and SUP-T1 T lymphoblastic cell line

We performed an unbiased global proteomic profiling to elucidate the protein expression profiles of resting (un-activated) and TCR- activated primary human CD4+- T cells (**Figure1A)** as well as the T cell lymphoblastic cell line SUP-T1. Peripheral Blood Mononuclear Cells (PBMCs) were isolated from two healthy donors, and CD4+ T cells were further purified using magnetic bead-based isolation (negative-isolation of "untouched" cells). Flow-cytometric analysis indicated a purity of >94% for both donors and in total less than 0.5% contaminating of myeloid origin (CD14+ or CD11c+ cells) or CD8+ T cells **(Figures 1B and 1C)**. Resting CD4+ T cells were frozen directly after isolation. For activated CD4+ T cell samples, TCR (plate-bound anti-CD3 antibody) and co-stimulatory (anti-CD28 antibody) signaling was induced for 72 hours before the samples were frozen.

LC-MS/MS analysis of resting and activated CD4+ T cell proteomes resulted in the identification of 5,237 proteins (**Supplementary Table 1**). The proteomic profiles of resting and activated CD4+ T cells from two donors were compared to see expression patterns using Principal Component Analysis (PCA). While resting cells from the donors clustered together in the PCA plot, activated cells revealed heterogeneous expression profiles between the two donors (**Figure 1D**), indicating that there were significant proteomic differences between them. A total of 1,119 were significantly altered between resting and activated states in both

donors (log_2 fold change ±2, p-value<0.05) **(Supplementary Figure 1A and 1B, Supplementary Table 1).** The top 10 differentially regulated proteins in activated CD4+ T cells from the two donors are provided in **Figures 1E and 1F**. Among the top 10 differentially regulated proteins, thymidylate synthetase (TYMS) and methylenetetrahydrofolate dehydrogenase (NADP+ dependent) 2 (MTHFD2) were found to upregulated in activated CD4+ T cells from both the donors while ATP synthase membrane subunit 6.8PL (ATP5MPL), azurocidin 1 (AZU1), granzyme K (GZMK) were found to be downregulated.

Known and novel molecular markers of resting and activated CD4+ T cells

We analyzed proteins characteristic of resting and activated CD4+ T cells. As expected, CD4 was uniformly expressed in both resting and activated CD4+ T cells (**Figure 2A**). CD8 protein was not identified in the current dataset, confirming the purity of the CD4+ T cell preparations. Protein expression profiles of the transcriptional regulator FOXP3 as well as interleukin (IL)-2 receptor α-chain IL2RA (CD25), major histocompatibility complex class II, DR alpha (HLA-DRA), CD40 ligand (CD40LG) and CD69 as hallmark markers of T cell activation were assessed. A marked increase in FOXP3, IL2RA, CD40LG, and CD69 protein expression was observed after 72 hours of activation compared to resting CD4+ T cells; HLA-DRA showed a minor increase in protein expression (**Figures 2B-2F).**

Next, we carried out gene ontology-based enrichment analysis of differentially expressed proteins in activated CD4+ T cells with respect to their resting/untreated counterparts. The two donors showed significant differences in the type of biological processes for which proteins were upregulated in CD4+ T cells after activation (**Figures 2G and 2H**). However, "housekeeping" processes pertaining to cell cycle, mitosis and DNA replication were commonly enhanced in both donors. The biological processes enriched for downregulated proteins were mostly similar for both donors and consisted mainly of proteins involved in neutrophil activation (**Supplementary figures 2A and 2B**).

Furthermore, a detailed comparison of proteins differentially expressed in activated CD4+ T cells compared to resting CD4+ T cells was carried out. Gene sets derived from the Molecular Signatures Database (MSigDB) were used to obtain insights into signaling in the course of T cell activation and modulating effector lineage differentiation. First, we compared the list of differentially expressed proteins with master lists of proteins involved in T cell activation, regulation of T cell activation, and markers of Th cell lineages (**Figures 2I-K).** Increased expression of CD4+ T cell activation markers including basic leucine zipper ATF-like transcription factor (BATF), forkhead box P3 protein (FOXP3), Interferon-γ (IFNG), T-box transcription factor 21 (TBX21/T-Bet), interferon regulatory factor 4 (IRF4), CD81, galectin 9 (LGALS9), RELB proto-oncogene, NF-kB subunit (RELB) and Janus kinase 3 (JAK3) was observed in activated cells of both donors. On the contrary, proteins including BCL3 transcription coactivator (BCL3), zinc finger, and BTB domain containing 7B (ZBTB7B) revealed mixed patterns of expression between the two donors. Notably, the expression of SLAMF6 was decreased after activation.

Several proteins belonging to the CD family, such as CD47, CD74, CD81, CD70, and CD40LG, were increased in activated CD4+T cells from both donors (**Figure 2J**). Other described modulator/regulator proteins of T cell activation that were increased in activated CD4+ T cells from both donors include inducible T cell costimulator (ICOS), TNF receptor superfamily member 1B (TNFRSF1B), TNF receptor superfamily member 18 (TNFRSF18),

interferon regulatory factor 1 (IRF1), interferon regulatory factor 4 (IRF4), interleukin 2 receptor subunit alpha (IL2RA), cytotoxic T-lymphocyte associated protein 4 (CTLA4), and transferrin receptor (TFRC). However, proteins, including interleukin 7 receptor (IL7R), CD300A, spleen associated tyrosine kinase (SYK), and NFKB activating protein (NKAP) were decreased in activated CD4+ T cells compared to their resting counterparts.

A number of proteins described as associated with a Th1-type effector CD4+ T cell response were found upregulated after activation, especially in CD4+ T cells from donor 1 (**Figure 2K**). These included expression of the Th1 cell hallmark cytokine Interferon-γ (IFNG), signal transducer, and activator of transcription 4 (STAT4) and (T-bet/TBX21), which were increased in the case of both donors. In the case of Th2 markers, increased expression of STAT6 but not GATA3 transcription factors was observed 72 hours post-activation. In addition, Th2 effector cytokines (IL4,5,13) were not found. With respect to Th17 markers, STAT3 but not RORC TF increased in activated CD4+ T cells from both donors. However, one of the hallmark cytokines IL17F, but not IL17A, was found to be increased in both donors. The Treg markers -transcription factors STAT5A, STAT5B, and FOXP3 and TGFB1 effector cytokine were increased after activation, however, IL10 was not detected after activation. In addition, transcription factors for other lineages were found, including ICOS for TFH lineage, IRF4 for Th9 lineage were increased after activation. However, markers for Th22 were not detected. The expression of all markers for Th cell lineages were similar in both donors. These results suggest a mixed lineage phenotype in both donors.

Activation of CD4+ T cells influences processes and signaling pathways

Kinases and phosphatases constitute important classes of proteins mediating cell signaling and could provide mechanistic insights into T cell activation. Towards this end, we explore the expression profile of protein kinases and phosphatases in resting and activated CD4+ T cells (**Figures 3A,B**). Protein kinases including Aurora kinase B (AURKB), cyclin dependent kinases (CDK1 and CDK2), RIO kinases (RIOK1 and RIOK2), checkpoint kinase 1 (CHEK1), Janus kinase 3 (JAK3), serine/threonine kinase 17b (STK17B) and SRSF protein kinase 1 (SRPK1) were significantly upregulated (p-value<0.05) 72 hours post-activation in CD4+ T cells from both donors. On the contrary, cyclin dependent kinase 13 (CDK13), TBC1 domain containing kinase (TBCK), kinases belonging to MAP kinases (MAPKAPK3, MAP3K2, and MAPK9), microtubule affinity regulating kinase 3 (MARK3), SNF related kinase (SNRK), ribonuclease L (RNASEL) and spleen associated tyrosine kinase (SYK) were significantly downregulated in activated CD4+ T cells from both donors. In general, more protein kinases were upregulated in activated CD4+ T cells from donor 1 compared to donor 2. Protein kinases such as mitogen-activated protein kinase 8 (MAPK8), calcium/calmodulin-dependent protein kinase ID (CAMK1D), mitogen-activated protein kinase 6 (MAPK6), PEAK1 related, kinase-activating pseudokinase 1 (PRAG1), TRAF2 and NCK interacting kinase (TNIK), misshapen like kinase 1 (MINK1) and ribosomal protein S6 kinase A4 (RPS6KA4) were only found to be upregulated in activated CD4+ T cells from donor 1 suggesting better activation of these cells. Among the phosphatases, the non-protein phosphatase- myotubularin related protein 9 (MTMR9) was found to be upregulated in activated CD4+ T cells, whereas the protein tyrosine phosphatase receptor type A (PTPRA) was found to be downregulated in activated CD4+ T cells from both donors. A significant decrease in the expression of protein tyrosine phosphatase receptor type J (PTPRJ), myotubularin related protein 12 (MTMR12), and synaptojanin 2 (SYNJ2) was observed in

activated CD4+ T cells from donor 2. These suggest that phosphatases were less impacted after activation in both donors.

We compared the proteomics data with MSigDB and literature-derived gene sets of the adaptive immune response, cytokines, cytokine receptors MAP kinases, and hypoxia and ROS markers (**Supplementary figure 3**). Besides Interferon-γ (IFNG), interleukin 17F (IL17F), and interleukin 2 receptor subunit alpha (IL2RA/CD25), we found interleukin 32 (IL32) and interleukin 2 receptor subunit gamma (IL2RG) to be overexpressed in activated CD4+ T cells, while interleukin 7 receptor (IL7R) was downregulated. Other upregulated proteins included bonafide cytokines that included platelet factor 4 (PF4/CXCL4), and proteins with predicted cytokine activities such as glomulin, FKBP associated protein (GLMN), CD40 ligand (CD40LG), nicotinamide phosphoribosyl transferase (NAMPT), and thymidine phosphorylase (TYMP). Protein markers of hypoxia, including perilipin 2 (PLIN2), high density lipoprotein binding protein (HDLBP), jumonji domain containing 6, arginine demethylase and lysine hydroxylase (JMJD6), hexokinase 2 (HK2), ilvB acetolactate synthase like (ILVBL), solute carrier family 2 member 1 (SLC2A1), and prolyl 4-hydroxylase subunit alpha 1 (P4HA1), were found to be upregulated in activated CD4+ T cells of both donors. Further, ROS markers apolipoprotein E (APOE) was found to be increased in expression in activated T cells while neutrophil cytosolic factor 2 (NCF2), ring finger protein 7 (RNF7), myeloperoxidase (MPO), and thioredoxin reductase 2 (TXNRD2) were found to be decreased. In summary, activated CD4+ T cells showed classical markers of adaptive immune responses, while the increased hypoxia markers in response to activation may be a result of increased nutritional needs of activated CD4+ T cells.

Comparison of proteomic data from resting and activated CD4+ T cell with genesets involved in carbohydrate, lipid, and amino acid metabolism was carried out (**Supplementary figure 4**). Comparison with proteins involved in glycolysis/gluconeogenesis identified that hexokinase 2 (HK2) was upregulated in activated cells, while aldehyde dehydrogenase 2 family member (ALDH2), fructose-bisphosphatase 2 (FBP2), and hexokinase 3 (HK3) were downregulated in activated CD4+ T cells. A significant amount of proteins involved in lipid metabolism were found to be increased in activated CD4+ T cells. These included acyl-CoA oxidase 1 (ACOX1), holocytochrome c synthase (HCCS), 3-hydroxy-3-methylglutaryl-CoA synthase 1 (HMGCS1), ELOVL fatty acid elongase 5 (ELOVL5), retinol saturase (RETSAT), isopentenyl-diphosphate delta isomerase (IDI1), fatty acid synthase (FASN), heat shock protein family H (Hsp110) member 1 (HSPH1), and ubiquitin conjugating enzyme E2 L6 (UBE2L6). Further, we also compared the proteomics data with proteins involved in amino acid metabolism. Amino acid metabolism proteins, including deoxyhypusine synthase (DHPS), pyrroline-5-carboxylate reductase 1 (PYCR1), folylpolyglutamate synthase (FPGS), methionyl-tRNA synthetase 2, mitochondrial (MARS2), fumarylacetoacetate hydrolase (FAH), solute carrier family 7 member 5 (SLC7A5), and tryptophanyl-tRNA synthetase 1 (WARS), were found to be upregulated in activated CD4+ T cells, while guanidinoacetate N-methyltransferase (GAMT) was found to be downregulated. However, several proteins pertaining to oxidative phosphorylation showed mixed patterns of expression. In summary, while several proteins for aa and lipid metabolism were upregulated after activation, a mixed expression pattern between resting and activated CD4+ T cells were observed for oxidative phos and glycolysis/gluconeogenesis proteins. We also looked at the changes in the expression of markers of the cell cycle, apoptosis, autophagy, and phagocytosis (**Supplementary figure 5**). Several proteins belonging to these processes were upregulated in activated CD4+ T cells indicating changes in cellular activity and cell proliferation in response to activation.

Pathway enrichment analysis of proteins differentially expressed in activated CD4+ T cells from both the donors revealed several pathways, such as Interferon signaling, cell cycle pathways, and nucleotide metabolism, to be enriched in activated CD4+ T cells (**Figure 3C)**. This is in line with reports suggesting increased cytokine-mediated differentiation and increased proliferation of activated CD4+ T cells.

Activation of CD4+ T cells influences signaling networks

Interactome analysis of proteins that were upregulated during activation of primary human CD4+ T cells was carried out on our datasets to identify critical regulatory hubs. The protein-protein interaction network was generated from the set of proteins upregulated in activated CD4+ T cells from both donors compared to non-activated CD4+ T cells using Cytoscape, and network topology parameters were calculated (**Figure 4**, **Supplementary Table 2**). The between centrality and degree measures were used to visualize the network and identify the highly connected nodes. Proteins with high between centrality measures included the proliferation marker - marker of proliferation Ki-67 (MKI67), cell cycle proteins including cyclin dependent kinase 1 (CDK1), cyclin dependent kinase 2 (CDK2), cell cycle associated protein 1 (CAPRIN1) and cell division cycle 20 (CDC20), the methyltransferase tRNA methyltransferase 1 (TRMT1), the ubiquitin transferase ubiquitin conjugating enzyme E2 L6 (UBE2L6), protein kinases aurora kinase B (AURKB) and RIO kinase 2 (RIOK2), interferon regulatory factor 1 (IRF1), forkhead box P3 (FOXP3), Interferon-γ (IFNG), intercellular adhesion molecule 2 (ICAM2), clusterin (CLU) and mini-chromosome maintenance proteins (MCM) including MCM2, MCM3, MCM4, MCM5, MCM5, and MCM7. These proteins probably represent regulatory hubs of CD4+ T cell activation and need to be investigated further.

Changes in expression levels of immune checkpoint proteins in activated/resting CD4+ T cells

The complete activation of CD4+ T cells depends on signals from the TCR (signal 1) and antigen-independent co-stimulatory signals (signal 2). In our set-up, we provided both signal 1 (anti-CD3 stimulation) and signal 2 (anti-CD28 stimulation) to primary CD4+ T cells for 72 hours. However, CD4+ T cell activation is tightly regulated by a range of co-stimulatory and co-inhibitory signaling receptors known as immune checkpoints. Immune checkpoints act as regulators of the immune system mediating interactions between T cells and other cells, such as APCs or tumor cells [5]. These inhibitory or stimulatory checkpoint pathways attenuate T cell activation and are essential for self-tolerance mechanisms and regulate the adaptive immune response [37, 38]. Immune checkpoints are considered as important immunotherapy targets, and checkpoint inhibitors against CTLA4, PD-1/PD-L1 have been approved for clinical use [39]. We compiled a list of proteins that constitute checkpoints of the immune system from publicly available literature [38, 40] and analyzed the levels of these in resting and activated CD4+T cells (**Figure 5**). Of the 16 immune checkpoints that were compiled, we identified ten checkpoints in the proteomics data. These included stimulatory checkpoint molecules such as CD27 (TNFRSF7), CD28, CD40LG (CD40L), CD96 (Part of TIGIT/CD96), inducible T cell costimulator (ICOS), TNF receptor superfamily member 4 (TNFRSF4/OX40), TNF receptor superfamily member 18 (TNFRSF18/GITR) and inhibitory checkpoint molecules including cytotoxic T-lymphocyte associated protein 4 (CTLA4), lymphocyte activating 3 (LAG3), and V-set immunoregulatory receptor (VSIR/VISTA/PD-1H).

Amongst these, CD27 (TNFRSF7), CD28, and VSIR (VISTA/PD-1H) proteins were found to be expressed at similar levels in both resting and activated CD4+ T cells, CD96 was expressed at higher levels in resting compared to activated CD4+ T cells. Interestingly, PD-1 (PDCD1) was neither detected in resting or activated CD4+ T cells in the current study. This may be because PD-1 is generally strongly expressed in late-stage exhausted T cells, such as those in the tumor environment and were not detected in our setup with strongly activated T cells at an early stage (72 hours). However, expression of the stimulatory checkpoint molecules CD40LG, ICOS, TNFRSF18 and TNFRSF4 (OX40) as well as the inhibitory immune checkpoint regulators CTLA4 and LAG3 was significantly upregulated 72 hours post-activation in CD4+ T cells. These results indicate that CD4+ T cells are highly responsive for distinct positive co-stimulatory signals 72 hours post-activation, but that at the same time, expression of certain inhibitory checkpoint molecules is induced and counter-acts the activation process.

Comparison of primary T cell data with proteomes of human lymphoblastic T cell lines

We also carried out a proteomic analysis of the SUP-T1 model T cell line in order to elucidate to what degree protein expression in SUP-T1 cells correlates to protein expression in resting (unactivated) primary CD4+ T cells. SUP-T1 cells are T cell lymphoblastic lymphoma cells do not express a functional TCR on their surface and were thus analyzed in a resting state (no TCR activation prior to analysis). LC-MS/MS analysis resulted in the generation of 167,863 peptide spectrum matches (PSM), which mapped 26,111 peptides corresponding to 4,815 proteins (**Supplementary Table 3**). We compared the proteomic profile of SUP-T1 cells with our dataset from resting primary CD4+ T cells and a published proteomic profile of another lymphoblastic T cell line, Jurkat A3 cells [36]. We found that 2,925 proteins or about 59% of resting proteins from resting primary T cells were also identified in SUP-T1and Jurkat cells (**Figure 6A, Supplementary Table 4**). Gene ontology-based enrichment revealed that the common processes across these cells included housekeeping processes such as RNA processing, translation initiation, and nuclear transport. We further assessed gene ontology-based enrichment for the proteins that were exclusive to each of the cells. The top enriched processes unique to resting primary CD4+ T cells included proteins assigned to the interferon gamma-mediated signaling pathway and T cell activation processes, suggesting that these processes were less represented in SUP-T1 and Jurkat cells. CD4 protein was found to be expressed in all cell types. Further examination into CD3 (a T cell co-receptor) expression revealed that CD3D and CD3E subunits were found to be expressed in all three cell types, while CD3G was found to be expressed in primary resting T cells and Jurkat but not SUP-T1 cells. However, CD28 expression was identified in resting and SUP-T1 cells, but not Jurkat cells (Supplementary Table 3). In addition to CD4, SUP-T1 cells also expressed CD8 (CD8B) albeit at lower levels. These findings suggest that there is a difference between T cell lines which may affect the phenotype under study.

Comparison of proteome data with previously published primary human and mouse CD4+ T cell datasets

We compared our proteomic profiles of human resting and activated CD4+ T cells with a previous study that performed proteomic analysis on mouse resting CD4+ T cells and Th1 cells [41] (**Supplementary Table 5**). The comparison revealed a substantial overlap of the proteins identified between both resting and activated mouse and human cells (**Figure 6B**). However, closer inspection of the pattern of expression with a similarity matrix showed a lower correlation between the mouse and human T cell datasets, indicating considerable

species-level differences in the protein expression profiles of both resting and activated CD4+ T cells (**Figure 6C**).

We also compared our acquired proteomic data on primary human CD4+ T cells with previously published proteomic datasets on human CD4+ T cells [30, 42, 43] (**Supplementary tables 6and 7**). Venn diagrams showed a large overlap of identified proteins across both resting and activated CD4+ T cells irrespective of the generation of mass spectrometers used (Figures **6D and 6E**). However, correlation matrices indicated a considerable heterogeneity in protein expression profiles between the different datasets. The proteomic profiles found by Rieckmann *et al.* [43] showed more similarity to the current study, while the proteome profiles from Gerner *et al.* [30] and Mitchell *et al.* [42] showed lower levels of correlation (**Figure 6F**). These suggest a heterogeneity across individuals and studies on T cell proteomic profiles.

Discussion

Primary human CD4+ T cells have been studied extensively pertaining to their role in adaptive immunity. Several omics-based studies have characterized the proteome of CD4+ T cells. However, despite these cells being studied in detail, the signaling mechanisms operating in these cells during steady-state and upon induction of activation is not entirely understood. To identify changes in the protein expression profiles of resting and TCR-activated CD4+ T cells, we performed a label-free quantitative proteomic analysis on primary human CD4+ T cells derived two donors. In addition, we carried out the proteomic analysis of SUP-T1 cells to compare and contrast proteome profiles of primary CD4+ T cells to a model T cell line. Our study indicated that during the course of CD4+ T cell activation, significant changes in the protein expression profile occur. We identified several proteins that were previously found to be differentially expressed in response to stimulation. Importantly, markers of CD4+ T cell activation along with their regulators and Th1-, Th2-, Th17-, and Treg-specific markers were found to be upregulated, suggesting the presence of potential transient hybrid cell types. This has been previously suggested by logical modeling-based simulations on T cell differentiation [44]. These findings suggest heterogeneity in CD4+ T helper cell types during activation and differentiation into terminally differentiated CD4+ T effector cells. This heterogeneity may arise due to varying stimuli that the donors were exposed to throughout life, the *in vitro* condition of cells, the single timepoint used in the study -72 hours, which probably represents an intermediate phase where the T cells may not be terminally differentiated into effector lineages. Further, the *in vitro* conditions used may not mimic the *in vivo* state where polarizing cytokine signals would usually arise from APCs.

Further, several protein kinases, cytokines, MAP kinases, and markers of adaptive immune response, ROS, and hypoxia were found to be upregulated. Several proteins belonging to lipid metabolism and amino acid metabolism were also found to upregulated in activated CD4+ T cells. This can be possibly be explained by the increasing cellular metabolic needs due to CD4+ T cell activation and proliferation. We identified several proteins belonging to the amino acid synthesis and transport to be upregulated in activated CD4+ T cells, indicating that uptake and utilization of nutrients are associated with T cell differentiation and function. Previously, researchers have suggested that amino acid transporters are essential for the normal differentiation and functioning of T cells [45]. In the current study, we identified the upregulation of sodium-dependent neutral AA transporters SLC1A4 (ASCT1), SLC1A5 (ASCT2), sodium-independent cationic AA transporters SLC7A1 and SLC3A2 (CD98). The transcript levels of SLC1A4 and SLC1A5, which are known to transport cysteine, were previously found to be expressed in activated CD4+ T cells [46]. T-cell activation by

CD3/CD28 stimulation has been shown to dramatically increase arginine transport. This transport was shown to be mediated by the transporter SLC7A1 (also known as HCAT1), which was shown to be upregulated at both transcript and protein levels during T cell activation [47]. Further, the regulated expression of amino acid transporters, including CD98, has been found to control the cell size of T lymphocytes [48]. In another study, the deletion of CD98 was found to cause a significant reduction of T cell expansion [49].

An additional objective of this study was to compare proteomes between primary CD4+ T cells and commonly used T cell lines including Jurkat and SUP-T1,. Comparison of the lists of identified proteins across the three cell types showed the majority of the proteome expressed in these cells was common, driving essential processes of transcription, translation, and transport. However, each of the cells also expressed proteomes exclusive to each cell type, which might be caused due to varying proteomic coverage and depth in the different experiments. Differences were observed in terms of CD3 and CD28 expression across these cell types, with CD3G not being identified in SUP-T1. This is in accordance with previous reports showing SUP-T1 cells to be CD3-negative[50, 51]. It is widely known that Jurkat cell lines are CD28+, and it not being detected in the previous proteomics data suggests low proteome coverage as a possible cause. Both SUP-T1 and Jurkat cell lines exhibited enrichment of processes such as double-strand break repair, histone modification, cell junction organizations, which could be due to the malignant nature of these lymphoblastic cell lines. In comparison, primary CD4+ T cells showed lower enrichment of repair processes. It can be concluded that these cell lines are essentially similar in terms of shared proteomes and can serve as useful models of resting primary CD4+ T cells. However, prior knowledge of the proteomes of these cell lines is desirable to study specific biological processes. Comparison of our data on CD4+ T cells with proteomic data from mouse CD4+ T cells showed lower levels of correlation, suggesting interspecies differences in CD4+ T cell activation, which may lead to poor translatability of findings of mouse-based experiments to the physiological state of T cell activation in humans. However, this needs to be validated and explored further.

We identified several potential regulatory hubs of CD4+ T cell activation using network analysis. These included proteins involved in inflammatory response, including VTN; CD40LG; IFNG; IL2RA; FN1; IL2RG; TNFRSF1B. The roles of IFNG, IRF1, and FOXP3 are well known in the context of T cell activation. Besides, we identified several proteins associated with the cell cycle, including CDK1, CDK2, CAPRIN1, CCNB1, and CDC20, to be potentially regulatory hubs of CD4+ T cell activation. Previous studies have suggested that cell cycle progression and cytokine signaling are closely linked during CD4+ effector T cell differentiation. While the initial expression of IL-2 was found to be independent of the cell cycle, effector cytokine expression such as IFNγ and IL-4 were found to increase after successive cell divisions [52]. Clonal expansion of resting CD4+ T cells after activation is known to be mediated by cyclic-dependent kinases and cyclins [53]. The cyclin-dependent kinases CDK1 and CDK2 and cyclin B1 (CCNB1) have been found to play an important role in the cell cycle with the cyclin B1-CDK1 complex playing a significant role to derive cell cycle progression [54, 55]. In T cells, CDK2 has been found to be critical for anergy, a primary mechanism for peripheral tolerance which causes diminished T cell activity in the absence of costimulatory signals from antigen recognition or the blocking of CD28 signaling [56]. Besides, CDK2-deficient CD4+ T cells were found to produce decreased levels of IL-2 and IFNγ in response to anti-CD3/anti-CD28 stimulation despite showing normal levels of activation, proliferation, and survival [57]. The upregulation of proteins involved in DNA replication such as MCM2-7 POLD3, POLA1, PCNA, and PRIM1; pyrimidine metabolism

proteins such as RRM1; UCK2; RRM2; TK1; TYMS; TYMP; and the marker KI67 (MKI67) during activation is explained the increased rate of cell proliferation. A few protein kinases such as RIOK2, AURKB, and PRKAB1 were found to be significantly upregulated in our datasets after activation of CD4+ T cells. Among these, RIOK2 and AURKB were found to have potential roles as regulatory hubs from the network analysis. Both RIOK2 and AURKB are associated with cell cycle activities. Aurora kinase B (AURKB) has been shown to regulate CD28-dependent T cell activation and proliferation [58]. RIO kinase 2 (RIOK2) is one of the members of the atypical protein kinase families [59]. RIOK2 is poorly studied compared to the other kinases; therefore, the biological mechanisms mediated by it are not well known. Over the years, a few papers have explored the role of RIOK2 in the context of the cell cycle. A study by Read and colleagues investigated a *Drosophila* glioblastoma model and discovered the Akt-dependent overexpression of RIOK1 and RIOK2 in glioblastoma cells [60]. Further, the study also found that the decreased expression of these kinases caused aberrant Akt signaling and resulted in cell cycle and apoptosis [60]. A recent study identified RIOK2 silencing in glioma cells inhibited cell migration and invasion [61]. RIOK2 has also been found to be essential for ribosome biogenesis [62, 63], which in turn is regulated in a cell cycle-dependent fashion [64]. However, there are no previous reports of RIOK2 being associated with T cell activation. While the modulatory role of sveral of these potential regulatory hubs in T cell activation is well known, others such as RIOK2 need to be studied further.

Previous reports have shown that CD4+ T cell activation results in substantial remodeling of the mitochondrial proteome that, in turn, generates specialized mitochondria with significant induction of the one-carbon metabolism pathway [65]. Defective one-carbon metabolism has been shown to result in defective resting T cell activation in aged mice [66]. In the current study, we identified several proteins belonging to the One carbon pool by folate pathway induced in CD4+ T cells after activation, including dihydrofolate reductase (DHFR), methylenetetrahydrofolate dehydrogenase (NADP+ dependent) 1 like (MTHFD1L), methylenetetrahydrofolate dehydrogenase (NADP+ dependent) 2, methenyltetrahydrofolate cyclohydrolase (MTHFD2), and thymidylate synthetase (TYMS). This confirms the previous findings of mitochondrial remodeling after CD4+ T cell activation.

We also identified heterogeneity in the levels of CD4+ T cell activation markers present in the cells from two donors. In our study, cells from donor 1 were observed to show more markers of activation, suggesting better activation. Further, resting cells from Donor 1 showed higher levels of protein kinases and phosphatases. This could be attributed to a higher degree of variability among primary donors with respect to their age, immune status, and recent exposure to infection. Comparison of CD4+ T cell proteomic profiles with other previously published studies also indicated considerable heterogeneity in proteomic expression profiles of both resting and activated T cells. The heterogeneity also extended to important regulatory molecules of the adaptive immune response, such as immune checkpoints.

Conclusions

The current study provides a new high-resolution proteomic snapshot of resting CD4+ T cells and after 72 hours of activation by TCR, together with a comparison to the proteome of T cell lines and resting/activated human/mouse CD4+ T cells. We confirmed several known T-cell activation-related processes such as IL-2 response, metabolic and signaling changes,cell cycle induction, differentiation into effector cells, among others. The current dataset also provides a

resource on checkpoint molecule expression (stimulatory/inhibitory) at this differentiation stage and implicates some proteins such as RIOK2 that previously have not been associated with CD4+ T cell activation. Thus the data generated from our study may contribute to a better understanding of the proteome transformations in primary CD4+ T cells during T cell activation and the comparability of the proteomes of primary human CD4+ T cells with T cell lines or mouse T cells. The data from our study here, together with other studies, may provide a foundation for developing therapeutic approaches to modulate CD4+ T cell functions.

Materials and Methods

Cells

Buffy coats from healthy blood donors were received from the Blood Bank (St Olav's Hospital, Trondheim) with approval by the Regional Committee for Medical and Health Research Ethics (REC Central, Norway, NO. 2009/2245). Peripheral Blood Mononuclear Cells (PBMCs) were isolated from Buffy coats by density gradient centrifugation (Lymphoprep, Axis-shield PoC). CD4+ T cells were isolated from PBMCs by a magnetic bead "negative" isolation procedure using the CD4+ T Cell Isolation Kit (Miltenyi Biotec) and LS columns (Miltenyi Biotec). CD4+ T cell purity was assessed by flow cytometry using anti-CD4 Alexa 700 (eBioscience) and anti-CD3 Brilliant Violet (BV) 785 (BioLegend) antibody staining. Data were acquired on a BD LSRII flow cytometer and analyzed using FlowJo software (FlowJo, LLC). For both donors, CD4+ T cell purity was > 94 % and cell preparations contained less than 0.1% CD8+ cells and less than 0.5% cells CD11c+ or CD14+ cells of myeloid origin (Figures **1B** and **1C**). SUP-T1 human T lymphoblast cells (ATCC) were cultured in RPMI 1640 (Gibco) supplemented with 10% FBS and penicillin/streptomycin (Thermo Fisher Scientific).

CD4+ T cell activation

For the unactivated (resting) CD4+ T cell samples, 1 x 10e7 CD4+ T cells from both donors were washed three times with PBS before the pellet was shock-frozen in liquid nitrogen and stored at -80 °C. For the activated CD4+ T cell samples, 1 x 10e7 CD4+ T cells from both donors were activated in anti-CD3 coated plates (clone OKT3, eBioscience, 5 µg/ml, 1 h) in the presence of 1 µg/ml anti-CD28 (clone CD28.2, eBioscience). CD4+ T cells were cultured for 72h in RPMI 1640 (Sigma-Aldrich), supplemented with 10% pooled human serum (The Blood Bank, St Olav's Hospital, Trondheim, Norway) at 37°C and 5% CO_2. CD4+ T cells were washed three times with PBS before the pellet was shock-frozen in liquid nitrogen and stored at -80.

Sample preparation of CD4+ T cell for proteomics

The cell lysates were reconstituted in 300 µl lysis buffer containing 4% sodium dodecyl sulfate (SDS) and 50mM triethyl ammonium bicarbonate (TEABC). They were sonicated three times for 10sec on ice, followed by heating at 90°C for 5 min. The lysate was further centrifuged at 12,000 rpm for 10 minutes. The concentration of protein was determined using bicinchoninic acid assay (BCA). The samples were subjected to in-solution trypsin digestion and subjected to strong cation exchange-based fractionation
Briefly, 200 µg of protein lysate of resting and activated CD4 were considered for trypsin digestion, where it was reduced by incubating in 10 mM dithiothreitol (DTT) at 60°C for 20 minutes and alkylated using 20 mM iodoacetamide (IAA) at room temperature for 10

minutes. This was followed by acetone precipitation for 6 hours, where the pellet was dissolved in 50mM TEABC. The lysate was then subjected for digestion using L-(tosylamido-2-phenyl) ethyl chloromethyl ketone (TPCK) treated trypsin (Worthington Biochemical Corporation, Lakewood, NJ, USA) at a final concentration of 1:20 (w/w) at 37°C overnight (~16 hrs). SCX fractionation was carried out as described previously [67].

Tandem mass spectrometry (MS/MS) analysis

The digested peptides were analyzed on Orbitrap Fusion Tribrid mass spectrometer interfaced with Easy-nLC-1200 (Thermo Scientific). Each fraction was reconstituted in 0.1% formic acid and loaded onto the trap column (75 um×2cm, nanoViper, 3um, 100A°) filled with C18 at a flow rate of 4 µl/min with Solvent A. The peptides were then resolved onto the analytical column (15 cm×50µm, nanoViper, 2µm) for 120 min. Data were acquired by using data-dependent acquisition mode at a scan range of 400-1600, in positive mode with a maximum injection time of 55 ms using an Orbitrap mass analyzer at a mass resolution of 120,000. MS/MS analysis was carried out at a scan range of 400-1,600. Top ten intense precursor ions were selected for each duty cycle and subjected to higher collision energy dissociation (HCD) with 35% normalized collision energy. The fragmented ions were detected using Orbitrap mass analyzer at a resolution of 120,000 with maximum injection time of 200ms. Internal calibration was carried out using a lock mass option (m/z 445.1200025) from ambient air.

Bioinformatics analysis of mass spectrometry data

The raw data obtained from mass spectrometry analysis were searched against the human Uniprot protein database (20,972 sequences, Downloaded from ftp://ftp.uniprot.org/ on July 3, 2019) using MaxQuant (v1.6.10.43) search algorithm. Trypsin was specified as the protease, and a maximum of two missed cleavages was specified. N-terminal protein acetylation and oxidation of methionine were set as variable modifications, while carbamidomethylation of cysteine was set as a fixed modification. The peptide length was set between 8-25 and precursor, and fragment mass tolerances were specified as 20ppm each. Decoy database search was used to calculate False Discovery Rate (FDR), which was set to 1% at PSM, protein, and peptide levels. The search results from MaxQuant were processed and label-free protein quantitation using Perseus (v 1.6.2.2, https://maxquant.net/perseus/) [68]. Briefly, intensity values were filtered, log-transformed, and fold-change calculations were performed. Perseus was also used to generate volcano and PCA plots.

Hypergeometric enrichment-based gene ontology and pathway analysis were carried out with R (R studio v1.2.1335, Bioconductor v 3.9.0) scripts using clusterProfiler (v.3.12.0) [69] and Reactome pathways [70] with ReactomePA package (v.1.28.0) [71]. The pathway enrichment parameters included 0.05 as p-value cut-off, Benjamini-Hochberg correction based p-value adjustment, minimum gene set size of 10, and q-value cut-off of 0.2. Pathways were plotted in R using ggplot2 package(v 3.3.0, https://cran.r-project.org/web/packages/ggplot2/).

The Gene Ontology (GO) enrichment for Biological processes was carried out using R with clusterProfiler. The GO enrichment parameters included 0.05 as p-value cut-off, Benjamini-Hochberg correction based p-value adjustment, minimum gene set size of 10. Gene lists for functions such as Cell cycle, phagocytosis, autophagy, apoptosis, hypoxia, adaptive immune response, and T cell activation were obtained from the Molecular Signatures Database (MSigDB, v7.0, https://www.gsea-msigdb.org/gsea/msigdb) [72]. Gene lists for metabolism was obtained from KEGG (https://www.genome.jp/kegg/), while genes list for reactive

oxygen species was compiled from the literature [73]. Protein kinase and phosphatase lists were obtained, as described previously [74]. Immune checkpoints receptors and their ligands were compiled from the literature [38, 40] and compared with the data from this study. Heatmaps were drawn using Morpheus (https://software.broadinstitute.org/morpheus/) with Euclidean complete linkage-based hierarchical clustering. Networks were generated using StringApp [75] in Cytoscape (version 3.7.1) [76] as previously described [77]. Briefly, proteins that were upregulated in both donors and significant were filtered and used to generate networks. The network properties were calculated using NetworkAnalyzer [78], and the network was visualized based on between centrality and degree values.

Isolation of SUP-T1 cell proteome and MS/MS analysis

The cell lysates of SUP-T1 was reconstituted in 300 µl lysis buffer containing 4% sodium dodecyl sulfate (SDS) and 50mM triethyl ammonium bicarbonate (TEABC). It was sonicated three times for 10 sec on ice, followed by heating at 90°C for 5 min. The lysate was further centrifuged at 12,000 rpm for 10 minutes. The concentration of protein was determined using bicinchoninic acid assay (BCA), giving a yield of 11.3 µg/ul. Protein lysate of 200 µg was considered for trypsin digestion where it was reduced by incubating in 10 mM dithiothreitol (DTT) at 60°C for 20 minutes and alkylated using 20 mM iodoacetamide (IAA) at room temperature for 10 minutes. This was followed by acetone precipitation for 6 hours where the pellet was dissolved in 50mM TEABC. The lysate was then subjected for digestion using L-(tosylamido-2-phenyl) ethyl chloromethyl ketone (TPCK) treated trypsin (Worthington Biochemical Corporation, Lakewood, NJ, USA) at a final concentration of 1:20 (w/w) at 37°C overnight (~16 hrs). SCX fractionation was carried out as described previously [67]. The digested peptides were analyzed on Orbitrap Fusion Tribrid mass spectrometer interfaced with Easy-nLC-1200 (Thermo Scientific). Each fraction was reconstituted in 0.1% formic acid and loaded onto the trap column (75 um×2cm, nanoViper, 3um, 100A°) filled with C18. The peptides were then resolved onto the analytical column (15 cm×50µm, nanoViper, 2µm) for 120 min at a flow rate of 250 nl/min. Data were acquired by using data-dependent acquisition mode at a scan range of 400-1600, in positive ion mode with a maximum injection time of 10 ms using an Orbitrap mass analyzer at a mass resolution of 120,000. MS/MS analysis was carried out at a scan range of 110-1,800. MS/MS analysis was carried out in Top Speed mode, and the precursor ions were subjected to higher collision energy dissociation (HCD) with 33% normalized collision energy. The fragmented ions were detected using Orbitrap mass analyzer at a resolution of 30,000 with maximum injection time of 200ms. Internal calibration was carried out using a lock mass option (m/z 445.1200025) from ambient air. Mass spectrometry derived data was searched against Human RefSeq 81 protein database in Proteome Discoverer 2.1 (Thermo Scientific, Bremen, Germany) using SEQUEST and Mascot (version 2.5.1, Matrix Science, London, UK) search algorithms. The parameters included trypsin as a proteolytic enzyme with maximum two missed cleavage where cysteine carbamidomethylation was specified as static modification and acetylation of protein N-terminus and oxidation of methionine was set as dynamic modifications. The length of 7 amino acids was set as minimum peptide length. The search was carried out with a precursor mass tolerance of 10 ppm and fragment mass tolerance of 0.05 Da. The data were searched against the decoy database with a 1 % FDR cut-off at the peptide level.

Comparison with published datasets

We carried out comparisons of the data from this study with previously published datasets to gain a better understanding of the proteomic landscapes of T cells. We downloaded protein

expression datasets of published studies and mapped them to gene symbols using a combination of g:Profiler (https://biit.cs.ut.ee/gprofiler/gost) [79], bioDBnet (https://biodbnet-abcc.ncifcrf.gov/db/db2db.php) [80] and UniProt ID mapping (https://www.uniprot.org/uploadlists/). Orthology conversion of mouse-to-human protein accessions was carried out using g:Orth function of g:Profiler and Homologene (https://www.ncbi.nlm.nih.gov/homologene) [81]. We compared proteomes of resting primary CD4+ T cells and SUP-T1 cells from the current dataset with a previously published proteome profile of Jurkat cells [36]. Hypergeometric enrichment-based gene ontology and pathway analysis were carried out with R (R studio v1.2.1335, Bioconductor v 3.9.0) scripts using clusterProfiler (v.3.12.0).

The datasets were subjected to z-score-based normalization using the scale function of base R (v3.6.0) and merged to create matrices. The datasets were then subjected to quantile normalization using normalizeBetweenArrays feature of limma (v3.40.6) to account for data distribution skewness between multiple datasets.

Data availability

Mass spectrometry-derived raw data were deposited to the ProteomeXchange Consortium (http://proteomecentral.proteomexchange.org) via the PRIDE partner repository [82, 83]. The data can be accessed using the dataset identifiers PXD015872 for CD4+ T cell data and. PXD021272 for SUP-T1 cell data.

Figure Legends

Figure 1. A. Workflow for the comparative proteomics analysis of resting and activated primary human CD4+ T cells as well as SUP-T1 lymphoma T cells. Primary human CD4+ T cells were purified using magnetic beads (MACS cell separation) from PMBCs of healthy donors. Resting (unstimulated) CD4+ T cell samples were harvested (washed and shock-frozen) for protein extraction immediately after isolation. A fraction (1x10e7) CD4+ T cells were activated for 72h by anti-CD3/anti-CD28 stimulation before cells were harvested/shock-frozen for protein isolation. SUP-T1 cells were harvested from a cell line tissue culture. Resting CD4+ T cells, activated CD4+ T cells and SUP-T1 cell samples were subjected to protein extraction. Proteins were subjected to tryptic digestion. Peptide samples obtained were subjected to strong cation exchange chromatography followed by MS/MS analysis. **B and C.** Flow cytometric purity analysis of CD4+ T cell preparations. **B**. Donor 1 and **C.** Donor 2. Purified CD4+ T cells were stained with fluorescent antibodies for CD11c, CD14, CD3, CD8 and CD4. Both preparations contained > 94 % CD3+CD4+ T cells and (in total) less than 0.5% contaminating CD11c+, CD14+ or CD8+ cells. **D.** Principal Component Analysis (PCA) plot depicting common proteomic patterns in resting/resting CD4+ T cells and activated CD4+ T cells. **E.** & **F.** S-curve graphs showing the distribution of fold-changes in Donors 1 and 2 and the top differentially expressed proteins.

Figure 2. Protein expression levels of **A.** CD4 **B.** FOXP3 **C.** IL2RA (CD25), **D.** HLA-DRA, **E.** CD40LG, **F.** CD69 in resting (R) and activated (A) primary CD4+ T cells from Donor1 (D1) and Donor2 (D2). Enriched Biological Processes from proteins upregulated in **G.** Donor 1 and **H.** Donor 2 in response to activation. Heatmaps depicting **I.** CD4+ T cell activation markers, **J.** Regulators of T cell activation in CD4+ T cells and **K.** Markers of T cell lineages. Genesets for comparison of significantly changing proteins were obtained from MSigDB.

Figure 3. Heatmaps depicting changes in **A.** protein kinases and **B.**protein in CD4+ T cells in response to activation. Genesets for comparison of significantly changing proteins were obtained from MSigDB. **C.** Significantly changing signaling pathways in resting and activated CD4+ T cells after pathway enrichment using Reactome Pathways

Figure 4. Network analysis of proteins upregulated in primary activated CD4+ T cells in both donors. The Network analysis was carried out using Cytoscape, and network topology properties were calculated using NetworkAnalyzer. The between centrality and degree measures were used to visualize the relationship between nodes. Larger sizes of nodes from high betweenness centrality suggest potential regulatory hubs.

Figure 5. An illustration representing expression profiles of immune checkpoint regulators in resting and activated primary CD4+ T cells. The inset graphs for each protein provide log2(intensity) value-based abundances for resting (R) and CD3/CD28-activated (A) CD4+ T cells from Donor1 (D1) and Donor2 (D2). Legends indicate Significant (*, FDR≤0.05), Not significant (NS), Not detected (ND)

Figure 6. A. Comparison between proteomic profiles of primary resting CD4+ T cells, SUP-T1 cells and Jurkat cells (Wu *et al.*, 2007) and Gene ontology-based classification of biological processes of common proteins and proteins distinct to each cell type **B.** Comparison of identified proteins and **C.** Correlation matrix between mouse (Howden *et al.*) and human CD4+ T cells (current study). Comparison of lists of identified proteins with previous studies on **D.** Resting and **E.** Activated human CD4+ T cells. **F.** Correlation matrix

for proteomic profiles of resting and activated CD4+ T cells from the current study, Rieckmann *et al.*, Gerner *et al.*, and Mitchell *et al.*

Supporting Information
Supplementary figures

Supplementary Figure 1. A & B. Volcano plots depicting upregulated and downregulated proteins in Donor 1 and Donor 2 CD4+ T cells in response to activation.

Supplementary Figure 2 Enriched Biological Processes from proteins downregulated in **A.** Donor 1 and **B.** Donor 2 in response to activation

Supplementary Figure 3. Protein expression profiles of various protein classes in resting and activated CD4+ T cells. Heatmaps depicting intensity-based abundances for differential expressed proteins for A. Adaptive immune response B. Hypoxia markers C. Interleukins D. Other cytokines E. MAP kinases F. Markers of Reactive Oxygen Species (ROS)

Supplementary Figure 4. Protein expression profiles for metabolic pathways in resting and activated CD4+ T cells. Heatmaps depicting intensity-based abundances for differential expressed proteins for A. Glycolysis/Gluconeogenesis B. Amino acid metabolism C. Lipid metabolism D. Oxidative Phosphorylation

Supplementary Figure 5 Protein expression profiles for cellular processes in resting and activated CD4+ T cells. Heatmaps depicting intensity-based abundances for differential expressed proteins for A. Cell cycle markers B. Apoptosis C. Autophagy D. Phagocytosis

Supplementary tables

Supplementary Table 1. Proteins identified from Activated and Resting CD4+ T cells using MaxQuant and significantly changing proteins in Activated and Resting CD4+ T cells in Donor 1 and 2

Supplementary Table 2. Node properties of Cytoscape network generated from protein upregulated in activated primary CD4+ T cells

Supplementary Table 3. Proteins identified from proteomic analysis of SUP-T1 cells

Supplementary Table 4. Lists of proteins identified in Resting primary CD4+ T cells, SUP-T1 and Jurkat cells (Wu *et al.* (2007))

Supplementary Table 5. Comparison of current human CD4+ T-cell proteomics dataset with mouse CD4+ Tcell proteomics data (Howden *et al.*)

Supplementary Table 6. Comparison of current CD4+ T-cell proteomics dataset with previous proteomic studies

Supplementary Table 7. Lists of proteins identified from the current study and previous studies on CD4+ T-cell proteomics

Funding: This work was funded by the Research Council of Norway (FRIMEDBIO "Young Research Talent" Grant 263168 to R.K.K.; and Centres of Excellence Funding Scheme Project 223255/F50 to CEMIR), Onsager fellowship from NTNU (to R.K.K.).

Acknowledgments: We thank the authors of the datasets used in this study for making their data publicly available.

Conflicts of Interest: The authors declare no conflict of interest

Abbreviations

AA	Amino Acid
FDR	False Discovery Rate
GO	Gene Ontology
KEGG	Kyoto Encyclopedia of Genes and Genomes
MACS	Magnetic-Activated Cell Sorting
NCBI	National Center for Biotechnology Information
PBMC	Peripheral Blood Mononuclear Cell
PSM	Peptide Spectrum Match
SDS	Sodium Dodecyl Sulphate
TCR	T cell receptor
TEABC	Triethyl ammonium bicarbonate
Th cells	T helper cells
TPCK	L-(tosylamido-2-phenyl) ethyl chloromethyl ketone

References

1. Luckheeram RV, Zhou R, Verma AD, Xia B. CD4(+)T cells: differentiation and functions. Clin Dev Immunol. 2012;2012:925135.
2. Famili F, Wiekmeijer AS, Staal FJ. The development of T cells from stem cells in mice and humans. Future Sci OA. 2017;3(3):FSO186.
3. Mondino A, Khoruts A, Jenkins MK. The anatomy of T-cell activation and tolerance. Proc Natl Acad Sci U S A. 1996;93(6):2245-52.
4. Hwang JR, Byeon Y, Kim D, Park SG. Recent insights of T cell receptor-mediated signaling pathways for T cell activation and development. Exp Mol Med. 2020;52(5):750-61.
5. Qin S, Xu L, Yi M, Yu S, Wu K, Luo S. Novel immune checkpoint targets: moving beyond PD-1 and CTLA-4. Mol Cancer. 2019;18(1):155.
6. Mosmann TR, Cherwinski H, Bond MW, Giedlin MA, Coffman RL. Two types of murine helper T cell clone. I. Definition according to profiles of lymphokine activities and secreted proteins. J Immunol. 1986;136(7):2348-57.
7. Geginat J, Paroni M, Maglie S, Alfen JS, Kastirr I, Gruarin P, De Simone M, Pagani M, Abrignani S. Plasticity of human CD4 T cell subsets. Front Immunol. 2014;5:630.

8. Raphael I, Nalawade S, Eagar TN, Forsthuber TG. T cell subsets and their signature cytokines in autoimmune and inflammatory diseases. Cytokine. 2015;74(1):5-17.
9. Christie D, Zhu J. Transcriptional regulatory networks for CD4 T cell differentiation. Curr Top Microbiol Immunol. 2014;381:125-72.
10. Oestreich KJ, Weinmann AS. Master regulators or lineage-specifying? Changing views on CD4+ T cell transcription factors. Nat Rev Immunol. 2012;12(11):799-804.
11. Berger EA, Doms RW, Fenyo EM, Korber BT, Littman DR, Moore JP, Sattentau QJ, Schuitemaker H, Sodroski J, Weiss RA. A new classification for HIV-1. Nature. 1998;391(6664):240.
12. Balasubramaniam M, Pandhare J, Dash C. Immune Control of HIV. J Life Sci (Westlake Village). 2019;1(1):4-37.
13. Okoye AA, Picker LJ. CD4(+) T-cell depletion in HIV infection: mechanisms of immunological failure. Immunol Rev. 2013;254(1):54-64.
14. Geldmacher C, Koup RA. Pathogen-specific T cell depletion and reactivation of opportunistic pathogens in HIV infection. Trends Immunol. 2012;33(5):207-14.
15. Hirahara K, Nakayama T. CD4+ T-cell subsets in inflammatory diseases: beyond the Th1/Th2 paradigm. Int Immunol. 2016;28(4):163-71.
16. Chemin K, Gerstner C, Malmstrom V. Effector Functions of CD4+ T Cells at the Site of Local Autoimmune Inflammation-Lessons From Rheumatoid Arthritis. Front Immunol. 2019;10:353.
17. Zhao Y, Lin L, Li J, Xiao Z, Chen B, Wan L, Li M, Wu X, Hin Cho C, Shen J. CD4(+) T cells in obesity and obesity-associated diseases. Cell Immunol. 2018;332:1-6.
18. Antony PA, Piccirillo CA, Akpinarli A, Finkelstein SE, Speiss PJ, Surman DR, Palmer DC, Chan CC, Klebanoff CA, Overwijk WW, Rosenberg SA, Restifo NP. CD8+ T cell immunity against a tumor/self-antigen is augmented by CD4+ T helper cells and hindered by naturally occurring T regulatory cells. J Immunol. 2005;174(5):2591-601.
19. Williams MA, Tyznik AJ, Bevan MJ. Interleukin-2 signals during priming are required for secondary expansion of CD8+ memory T cells. Nature. 2006;441(7095):890-3.
20. Janssen EM, Lemmens EE, Wolfe T, Christen U, von Herrath MG, Schoenberger SP. CD4+ T cells are required for secondary expansion and memory in CD8+ T lymphocytes. Nature. 2003;421(6925):852-6.
21. Laidlaw BJ, Craft JE, Kaech SM. The multifaceted role of CD4(+) T cells in CD8(+) T cell memory. Nat Rev Immunol. 2016;16(2):102-11.
22. Smith CM, Wilson NS, Waithman J, Villadangos JA, Carbone FR, Heath WR, Belz GT. Cognate CD4(+) T cell licensing of dendritic cells in CD8(+) T cell immunity. Nat Immunol. 2004;5(11):1143-8.
23. Takeuchi A, Badr Mel S, Miyauchi K, Ishihara C, Onishi R, Guo Z, Sasaki Y, Ike H, Takumi A, Tsuji NM, Murakami Y, Katakai T, Kubo M, Saito T. CRTAM determines the CD4+ cytotoxic T lymphocyte lineage. J Exp Med. 2016;213(1):123-38.
24. Xie Y, Akpinarli A, Maris C, Hipkiss EL, Lane M, Kwon EK, Muranski P, Restifo NP, Antony PA. Naive tumor-specific CD4(+) T cells differentiated in vivo eradicate established melanoma. J Exp Med. 2010;207(3):651-67.
25. Quezada SA, Simpson TR, Peggs KS, Merghoub T, Vider J, Fan X, Blasberg R, Yagita H, Muranski P, Antony PA, Restifo NP, Allison JP. Tumor-reactive CD4(+) T cells develop cytotoxic activity and eradicate large established melanoma after transfer into lymphopenic hosts. J Exp Med. 2010;207(3):637-50.
26. Matsuzaki J, Tsuji T, Luescher IF, Shiku H, Mineno J, Okamoto S, Old LJ, Shrikant P, Gnjatic S, Odunsi K. Direct tumor recognition by a human CD4(+) T-cell subset potently mediates tumor growth inhibition and orchestrates anti-tumor immune responses. Sci Rep. 2015;5:14896.

27. Reed CM, Cresce ND, Mauldin IS, Slingluff CL, Jr., Olson WC. Vaccination with Melanoma Helper Peptides Induces Antibody Responses Associated with Improved Overall Survival. Clin Cancer Res. 2015;21(17):3879-87.
28. Gnjatic S, Atanackovic D, Jager E, Matsuo M, Selvakumar A, Altorki NK, Maki RG, Dupont B, Ritter G, Chen YT, Knuth A, Old LJ. Survey of naturally occurring CD4+ T cell responses against NY-ESO-1 in cancer patients: correlation with antibody responses. Proc Natl Acad Sci U S A. 2003;100(15):8862-7.
29. Marchingo JM, Cantrell DA. The active inner life of naive T cells. Nat Immunol. 2020;21(8):827-8.
30. Gerner MC, Niederstaetter L, Ziegler L, Bileck A, Slany A, Janker L, Schmidt RLJ, Gerner C, Del Favero G, Schmetterer KG. Proteome Analysis Reveals Distinct Mitochondrial Functions Linked to Interferon Response Patterns in Activated CD4+ and CD8+ T Cells. Front Pharmacol. 2019;10:727.
31. Tan H, Yang K, Li Y, Shaw TI, Wang Y, Blanco DB, Wang X, Cho JH, Wang H, Rankin S, Guy C, Peng J, Chi H. Integrative Proteomics and Phosphoproteomics Profiling Reveals Dynamic Signaling Networks and Bioenergetics Pathways Underlying T Cell Activation. Immunity. 2017;46(3):488-503.
32. Duguet F, Locard-Paulet M, Marcellin M, Chaoui K, Bernard I, Andreoletti O, Lesourne R, Burlet-Schiltz O, Gonzalez de Peredo A, Saoudi A. Proteomic Analysis of Regulatory T Cells Reveals the Importance of Themis1 in the Control of Their Suppressive Function. Mol Cell Proteomics. 2017;16(8):1416-32.
33. Kubach J, Lutter P, Bopp T, Stoll S, Becker C, Huter E, Richter C, Weingarten P, Warger T, Knop J, Mullner S, Wijdenes J, Schild H, Schmitt E, Jonuleit H. Human CD4+CD25+ regulatory T cells: proteome analysis identifies galectin-10 as a novel marker essential for their anergy and suppressive function. Blood. 2007;110(5):1550-8.
34. Mohammad I, Nousiainen K, Bhosale SD, Starskaia I, Moulder R, Rokka A, Cheng F, Mohanasundaram P, Eriksson JE, Goodlett DR, Lahdesmaki H, Chen Z. Quantitative proteomic characterization and comparison of T helper 17 and induced regulatory T cells. PLoS Biol. 2018;16(5):e2004194.
35. Wolf T, Jin W, Zoppi G, Vogel IA, Akhmedov M, Bleck CKE, Beltraminelli T, Rieckmann JC, Ramirez NJ, Benevento M, Notarbartolo S, Bumann D, Meissner F, Grimbacher B, Mann M, Lanzavecchia A, Sallusto F, Kwee I, Geiger R. Dynamics in protein translation sustaining T cell preparedness. Nat Immunol. 2020;21(8):927-37.
36. Wu L, Hwang SI, Rezaul K, Lu LJ, Mayya V, Gerstein M, Eng JK, Lundgren DH, Han DK. Global survey of human T leukemic cells by integrating proteomics and transcriptomics profiling. Mol Cell Proteomics. 2007;6(8):1343-53.
37. Marin-Acevedo JA, Dholaria B, Soyano AE, Knutson KL, Chumsri S, Lou Y. Next generation of immune checkpoint therapy in cancer: new developments and challenges. J Hematol Oncol. 2018;11(1):39.
38. Pardoll DM. The blockade of immune checkpoints in cancer immunotherapy. Nat Rev Cancer. 2012;12(4):252-64.
39. Darvin P, Toor SM, Sasidharan Nair V, Elkord E. Immune checkpoint inhibitors: recent progress and potential biomarkers. Exp Mol Med. 2018;50(12):1-11.
40. Zahavi DJ, Weiner LM. Targeting Multiple Receptors to Increase Checkpoint Blockade Efficacy. Int J Mol Sci. 2019;20(1).
41. Howden AJM, Hukelmann JL, Brenes A, Spinelli L, Sinclair LV, Lamond AI, Cantrell DA. Quantitative analysis of T cell proteomes and environmental sensors during T cell differentiation. Nat Immunol. 2019;20(11):1542-54.
42. Mitchell CJ, Getnet D, Kim MS, Manda SS, Kumar P, Huang TC, Pinto SM, Nirujogi RS, Iwasaki M, Shaw PG, Wu X, Zhong J, Chaerkady R, Marimuthu A, Muthusamy B,

Sahasrabuddhe NA, Raju R, Bowman C, Danilova L, Cutler J, Kelkar DS, Drake CG, Prasad TS, Marchionni L, Murakami PN, Scott AF, Shi L, Thierry-Mieg J, Thierry-Mieg D, Irizarry R, Cope L, Ishihama Y, Wang C, Gowda H, Pandey A. A multi-omic analysis of human naive CD4+ T cells. BMC Syst Biol. 2015;9:75.

43. Rieckmann JC, Geiger R, Hornburg D, Wolf T, Kveler K, Jarrossay D, Sallusto F, Shen-Orr SS, Lanzavecchia A, Mann M, Meissner F. Social network architecture of human immune cells unveiled by quantitative proteomics. Nat Immunol. 2017;18(5):583-93.

44. Naldi A, Carneiro J, Chaouiya C, Thieffry D. Diversity and plasticity of Th cell types predicted from regulatory network modelling. PLoS Comput Biol. 2010;6(9):e1000912.

45. Ren W, Liu G, Yin J, Tan B, Wu G, Bazer FW, Peng Y, Yin Y. Amino-acid transporters in T-cell activation and differentiation. Cell Death Dis. 2017;8(3):e2655.

46. Levring TB, Hansen AK, Nielsen BL, Kongsbak M, von Essen MR, Woetmann A, Odum N, Bonefeld CM, Geisler C. Activated human CD4+ T cells express transporters for both cysteine and cystine. Sci Rep. 2012;2:266.

47. Werner A, Amann E, Schnitzius V, Habermeier A, Luckner-Minden C, Leuchtner N, Rupp J, Closs EI, Munder M. Induced arginine transport via cationic amino acid transporter-1 is necessary for human T-cell proliferation. Eur J Immunol. 2016;46(1):92-103.

48. Kelly AP, Finlay DK, Hinton HJ, Clarke RG, Fiorini E, Radtke F, Cantrell DA. Notch-induced T cell development requires phosphoinositide-dependent kinase 1. EMBO J. 2007;26(14):3441-50.

49. Cantor J, Slepak M, Ege N, Chang JT, Ginsberg MH. Loss of T cell CD98 H chain specifically ablates T cell clonal expansion and protects from autoimmunity. J Immunol. 2011;187(2):851-60.

50. Sandberg Y, Verhaaf B, van Gastel-Mol EJ, Wolvers-Tettero IL, de Vos J, Macleod RA, Noordzij JG, Dik WA, van Dongen JJ, Langerak AW. Human T-cell lines with well-defined T-cell receptor gene rearrangements as controls for the BIOMED-2 multiplex polymerase chain reaction tubes. Leukemia. 2007;21(2):230-7.

51. Burger R, Hansen-Hagge TE, Drexler HG, Gramatzki M. Heterogeneity of T-acute lymphoblastic leukemia (T-ALL) cell lines: suggestion for classification by immunophenotype and T-cell receptor studies. Leuk Res. 1999;23(1):19-27.

52. Bird JJ, Brown DR, Mullen AC, Moskowitz NH, Mahowald MA, Sider JR, Gajewski TF, Wang CR, Reiner SL. Helper T cell differentiation is controlled by the cell cycle. Immunity. 1998;9(2):229-37.

53. Chapman NM, Chi H. Hallmarks of T-cell Exit from Quiescence. Cancer Immunol Res. 2018;6(5):502-8.

54. Jang SH, Kim AR, Park NH, Park JW, Han IS. DRG2 Regulates G2/M Progression via the Cyclin B1-Cdk1 Complex. Mol Cells. 2016;39(9):699-704.

55. Jackman M, Lindon C, Nigg EA, Pines J. Active cyclin B1-Cdk1 first appears on centrosomes in prophase. Nat Cell Biol. 2003;5(2):143-8.

56. Wells AD, Morawski PA. New roles for cyclin-dependent kinases in T cell biology: linking cell division and differentiation. Nat Rev Immunol. 2014;14(4):261-70.

57. Chunder N, Wang L, Chen C, Hancock WW, Wells AD. Cyclin-dependent kinase 2 controls peripheral immune tolerance. J Immunol. 2012;189(12):5659-66.

58. Song J, Salek-Ardakani S, So T, Croft M. The kinases aurora B and mTOR regulate the G1-S cell cycle progression of T lymphocytes. Nat Immunol. 2007;8(1):64-73.

59. Manning G, Whyte DB, Martinez R, Hunter T, Sudarsanam S. The protein kinase complement of the human genome. Science. 2002;298(5600):1912-34.

60. Read RD, Fenton TR, Gomez GG, Wykosky J, Vandenberg SR, Babic I, Iwanami A, Yang H, Cavenee WK, Mischel PS, Furnari FB, Thomas JB. A kinome-wide RNAi screen in

Drosophila Glia reveals that the RIO kinases mediate cell proliferation and survival through TORC2-Akt signaling in glioblastoma. PLoS Genet. 2013;9(2):e1003253.
61. Song Y, Li C, Jin L, Xing J, Sha Z, Zhang T, Ji D, Yu R, Gao S. RIOK2 is negatively regulated by miR-4744 and promotes glioma cell migration/invasion through epithelial-mesenchymal transition. J Cell Mol Med. 2020;24(8):4494-509.
62. Ferreira-Cerca S, Sagar V, Schafer T, Diop M, Wesseling AM, Lu H, Chai E, Hurt E, LaRonde-LeBlanc N. ATPase-dependent role of the atypical kinase Rio2 on the evolving pre-40S ribosomal subunit. Nat Struct Mol Biol. 2012;19(12):1316-23.
63. Zemp I, Wild T, O'Donohue MF, Wandrey F, Widmann B, Gleizes PE, Kutay U. Distinct cytoplasmic maturation steps of 40S ribosomal subunit precursors require hRio2. J Cell Biol. 2009;185(7):1167-80.
64. Prakash V, Carson BB, Feenstra JM, Dass RA, Sekyrova P, Hoshino A, Petersen J, Guo Y, Parks MM, Kurylo CM, Batchelder JE, Haller K, Hashimoto A, Rundqivst H, Condeelis JS, Allis CD, Drygin D, Nieto MA, Andang M, Percipalle P, Bergh J, Adameyko I, Farrants AO, Hartman J, Lyden D, Pietras K, Blanchard SC, Vincent CT. Ribosome biogenesis during cell cycle arrest fuels EMT in development and disease. Nat Commun. 2019;10(1):2110.
65. Ron-Harel N, Santos D, Ghergurovich JM, Sage PT, Reddy A, Lovitch SB, Dephoure N, Satterstrom FK, Sheffer M, Spinelli JB, Gygi S, Rabinowitz JD, Sharpe AH, Haigis MC. Mitochondrial Biogenesis and Proteome Remodeling Promote One-Carbon Metabolism for T Cell Activation. Cell Metab. 2016;24(1):104-17.
66. Ron-Harel N, Notarangelo G, Ghergurovich JM, Paulo JA, Sage PT, Santos D, Satterstrom FK, Gygi SP, Rabinowitz JD, Sharpe AH, Haigis MC. Defective respiration and one-carbon metabolism contribute to impaired naive T cell activation in aged mice. Proc Natl Acad Sci U S A. 2018;115(52):13347-52.
67. Kulak NA, Pichler G, Paron I, Nagaraj N, Mann M. Minimal, encapsulated proteomic-sample processing applied to copy-number estimation in eukaryotic cells. Nat Methods. 2014;11(3):319-24.
68. Tyanova S, Temu T, Sinitcyn P, Carlson A, Hein MY, Geiger T, Mann M, Cox J. The Perseus computational platform for comprehensive analysis of (prote)omics data. Nat Methods. 2016;13(9):731-40.
69. Yu G, Wang LG, Han Y, He QY. clusterProfiler: an R package for comparing biological themes among gene clusters. OMICS. 2012;16(5):284-7.
70. Fabregat A, Jupe S, Matthews L, Sidiropoulos K, Gillespie M, Garapati P, Haw R, Jassal B, Korninger F, May B, Milacic M, Roca CD, Rothfels K, Sevilla C, Shamovsky V, Shorser S, Varusai T, Viteri G, Weiser J, Wu G, Stein L, Hermjakob H, D'Eustachio P. The Reactome Pathway Knowledgebase. Nucleic Acids Res. 2018;46(D1):D649-D55.
71. Yu G, He QY. ReactomePA: an R/Bioconductor package for reactome pathway analysis and visualization. Mol Biosyst. 2016;12(2):477-9.
72. Subramanian A, Tamayo P, Mootha VK, Mukherjee S, Ebert BL, Gillette MA, Paulovich A, Pomeroy SL, Golub TR, Lander ES, Mesirov JP. Gene set enrichment analysis: a knowledge-based approach for interpreting genome-wide expression profiles. Proc Natl Acad Sci U S A. 2005;102(43):15545-50.
73. Meguid NA, Ghozlan SAS, Mohamed MF, Ibrahim MK, Dawood RM, Din N, Abdelhafez TH, Hemimi M, Awady MKE. Expression of Reactive Oxygen Species-Related Transcripts in Egyptian Children With Autism. Biomark Insights. 2017;12:1177271917691035.
74. Subbannayya Y, Pinto SM, Bosl K, Prasad TSK, Kandasamy RK. Dynamics of Dual Specificity Phosphatases and Their Interplay with Protein Kinases in Immune Signaling. Int J Mol Sci. 2019;20(9).

75. Doncheva NT, Morris JH, Gorodkin J, Jensen LJ. Cytoscape StringApp: Network Analysis and Visualization of Proteomics Data. J Proteome Res. 2019;18(2):623-32.
76. Shannon P, Markiel A, Ozier O, Baliga NS, Wang JT, Ramage D, Amin N, Schwikowski B, Ideker T. Cytoscape: a software environment for integrated models of biomolecular interaction networks. Genome Res. 2003;13(11):2498-504.
77. Subbannayya Y, Pinto SM, Mohanty V, Dagamajalu S, Prasad TSK, Murthy KR. What Makes Cornea Immunologically Unique and Privileged? Mechanistic Clues from a High-Resolution Proteomic Landscape of the Human Cornea. OMICS. 2020;24(3):129-39.
78. Su G, Morris JH, Demchak B, Bader GD. Biological network exploration with Cytoscape 3. Curr Protoc Bioinformatics. 2014;47:8 13 1-24.
79. Raudvere U, Kolberg L, Kuzmin I, Arak T, Adler P, Peterson H, Vilo J. g:Profiler: a web server for functional enrichment analysis and conversions of gene lists (2019 update). Nucleic Acids Res. 2019;47(W1):W191-W8.
80. Mudunuri U, Che A, Yi M, Stephens RM. bioDBnet: the biological database network. Bioinformatics. 2009;25(4):555-6.
81. Coordinators NR. Database resources of the National Center for Biotechnology Information. Nucleic Acids Res. 2016;44(D1):D7-19.
82. Perez-Riverol Y, Csordas A, Bai J, Bernal-Llinares M, Hewapathirana S, Kundu DJ, Inuganti A, Griss J, Mayer G, Eisenacher M, Perez E, Uszkoreit J, Pfeuffer J, Sachsenberg T, Yilmaz S, Tiwary S, Cox J, Audain E, Walzer M, Jarnuczak AF, Ternent T, Brazma A, Vizcaino JA. The PRIDE database and related tools and resources in 2019: improving support for quantification data. Nucleic Acids Res. 2019;47(D1):D442-D50.
83. Vizcaino JA, Deutsch EW, Wang R, Csordas A, Reisinger F, Rios D, Dianes JA, Sun Z, Farrah T, Bandeira N, Binz PA, Xenarios I, Eisenacher M, Mayer G, Gatto L, Campos A, Chalkley RJ, Kraus HJ, Albar JP, Martinez-Bartolome S, Apweiler R, Omenn GS, Martens L, Jones AR, Hermjakob H. ProteomeXchange provides globally coordinated proteomics data submission and dissemination. Nat Biotechnol. 2014;32(3):223-6.

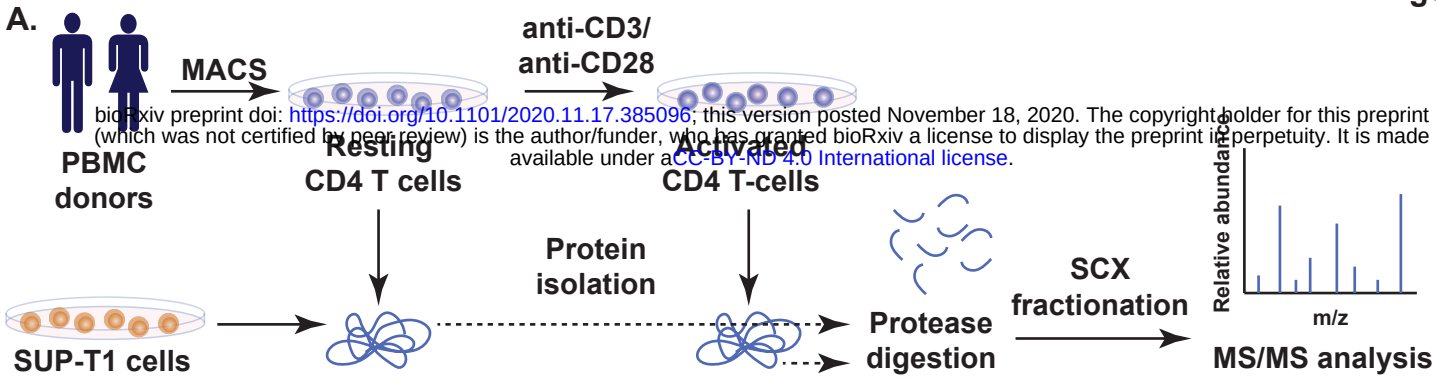

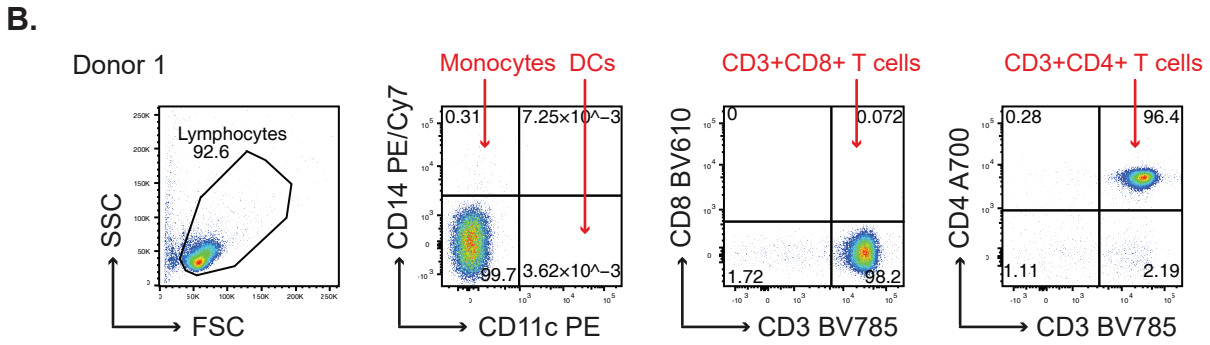

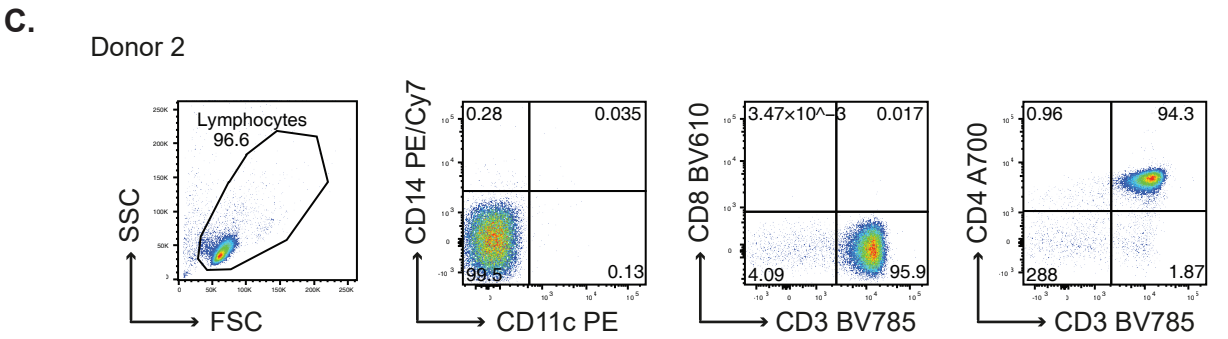

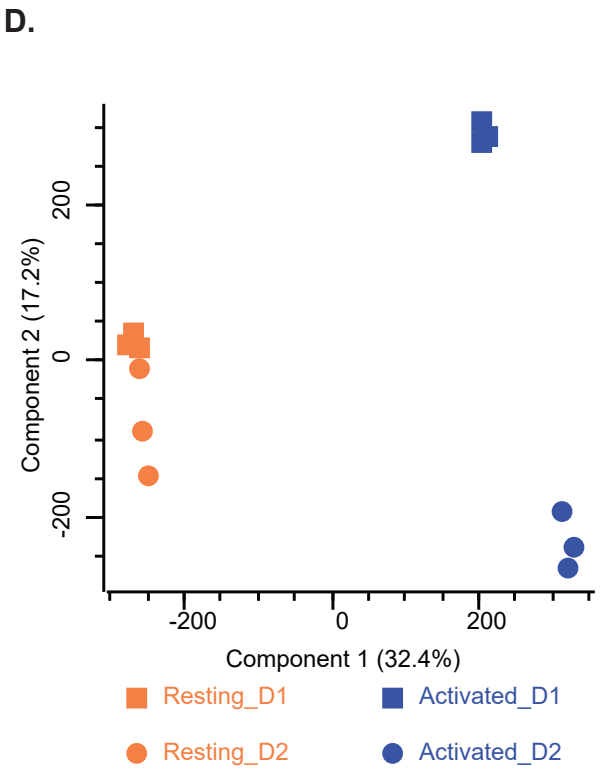

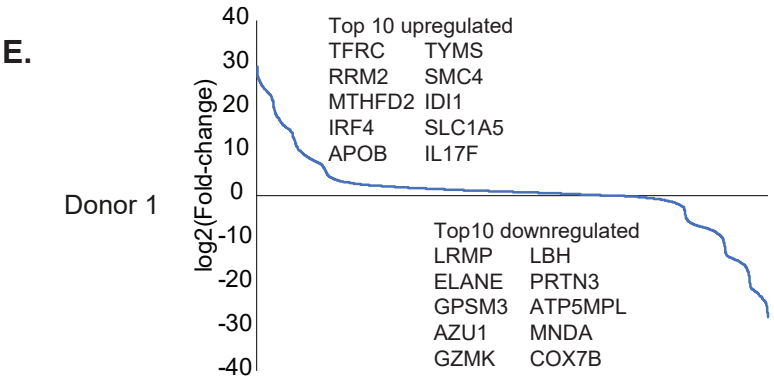

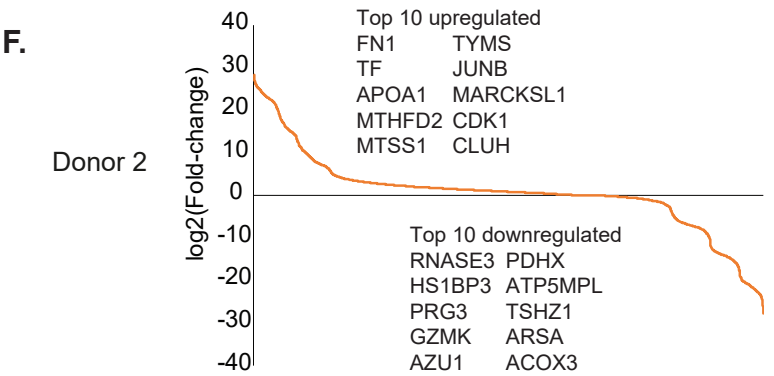

Figure 2

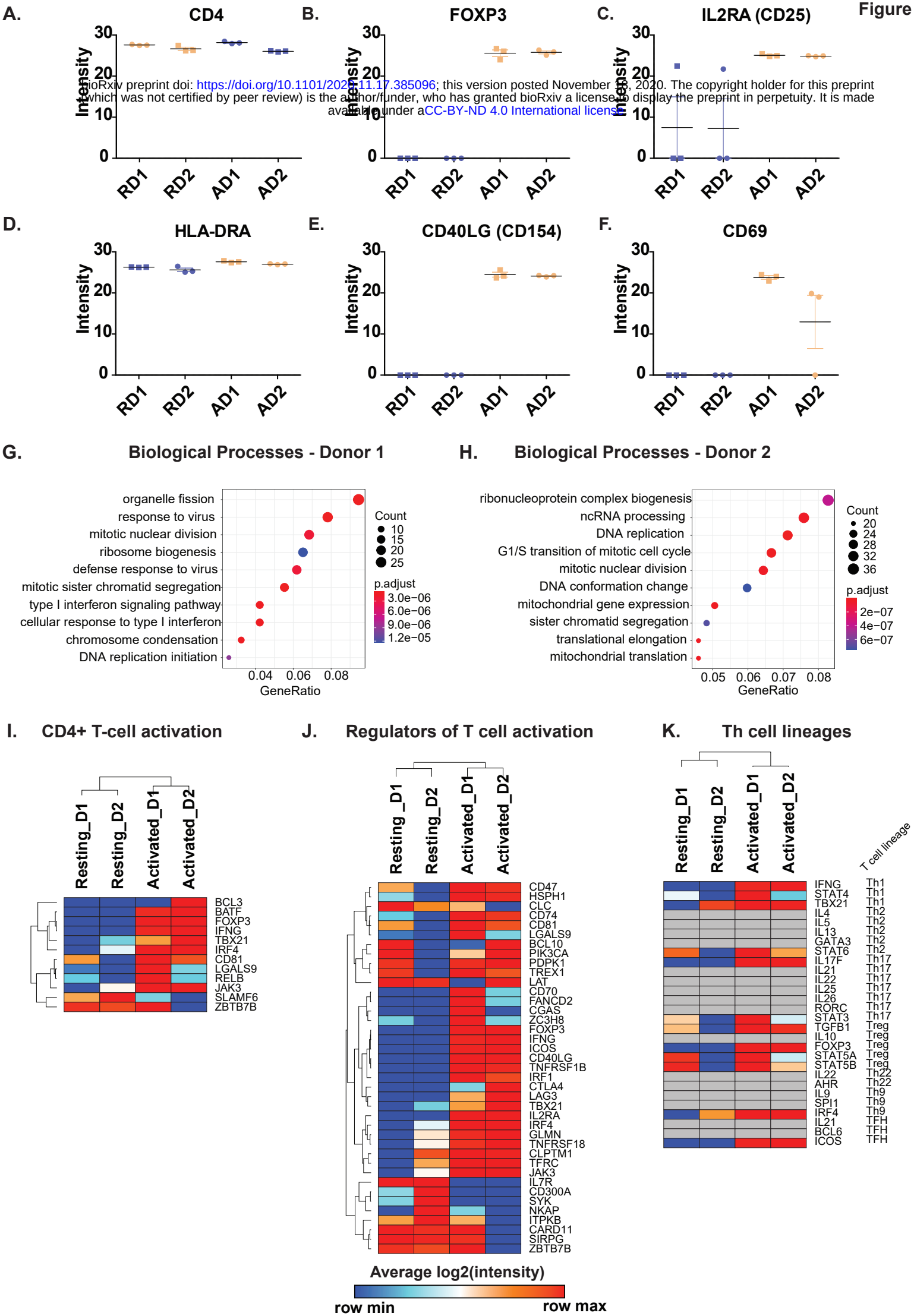

A.

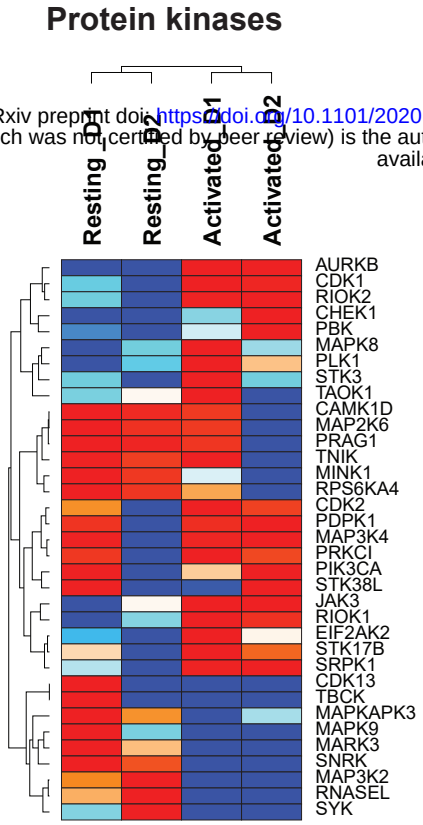

B.

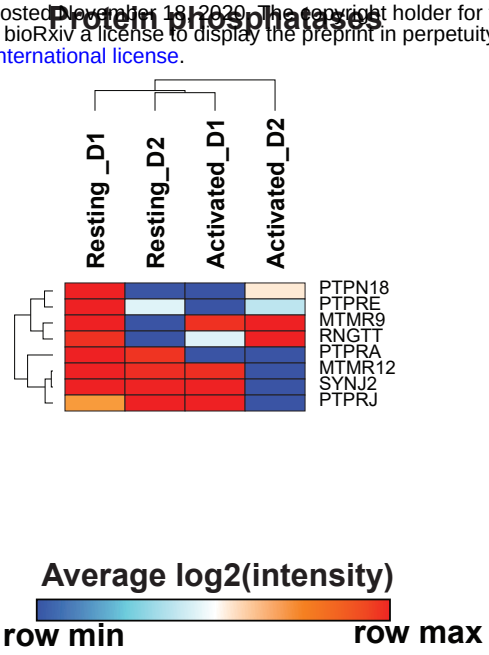

C.